Foreword

Rarely before has the field of nuclear medicine grown at such a pace as today. Reimbursement in many countries has led to a growing acceptance of PET and now PET-CT in the clinical setting and its full integration into clinical practice. At the same time, many new and promising target-specific radioligands have emerged in the research laboratory and await translation into the clinical environment. Once introduced into the clinic, they are likely to further transform the scope of nuclear medicine with substantial implications for patient care, including patient diagnosis and staging of disease and risk assessment. Moreover, they are likely to enhance treatment response monitoring and, importantly, facilitate tailoring of patient-specific treatment strategies.

Advances in imaging instrumentation have further accelerated the pace of growth in clinical nuclear medicine. Greater sensitivity together with higher spatial and temporal resolution capabilities has shortened clinical imaging times and thus increased patient throughput. It has also enhanced our ability to visualize and quantify normal functional processes, or altered, even when still subtle in magnitude in developing disease or when still confined to anatomically small regions. Importantly, PET-CT allows accurate localization of functional processes including rates of metabolism, receptor expression and activity, cell–cell or cell–tissue interactions, or events occurring at the molecular level. Functional parameters can thus be assigned to disease-related structural derangements. Finally, research in molecular imaging continues to produce a stream of novel, target-specific radioligands for probing molecular and cellular processes and promising to visualize and delineate cellular and molecular events at the onset of disease or in response to therapy. Many of these novel probes hold considerable promise for defining new targets for therapeutic strategies or, conversely, to serve as therapeutic agents themselves.

These impressive advances offer new and exciting opportunities for broadening the practice of nuclear medicine. Yet they also pose tremendous challenges to the clinician, especially as to how best apply the ever-growing array of imaging capabilities to patient care. The editors, Doctors Schober and Heindel deserve credit for providing us with a comprehensive and concisely written survey of the current state of clinical PET and PET-CT imaging. They have enlisted an outstanding team of contributors, all active clinicians in nuclear medicine, radiology, oncology, radiation therapy, neurology, or cardiology. As most of the contributors practice at the same academic medical center, they present a unified and coordinated approach to diagnostic imaging.

The text covers the full range of current PET and PET-CT applications, including those in neurology and cardiology and appropriately emphasizes applications in oncology. Importantly, the chapters adhere to a consistent structure and include a brief assessment of alternative imaging approaches such as MRI and CT, listing advantages and limitations, a feature which is especially useful for selecting the most effective and appropriate imaging approach and deciding when to use PET or PET-CT for solving a clinical question. I wish to congratulate the editors and contributors alike on this superb book, which serves as a readily accessible resource to the imaging clinician and as a well-organized, easily readable, and well-illustrated introduction to PET-CT for the beginner.

Heinrich R. Schelbert
George V. Taplin Professor
David Geffen School of Medicine at UCLA
University of California at Los Angeles
Los Angeles, CA, USA

Malignant Pleural Mesothelioma

Introduction and Staging

Malignant pleural mesothelioma (MPM) accounts for less than 2% of all thoracic tumors but is the most common pleural malignancy. The likelihood of contracting this disease is increased approx. 100-fold by asbestos exposure (Sohrab and Konietzko 2002). Generally a period of 20–30 years elapses between the initial asbestos exposure and manifestation of disease. In many countries the manufacture and processing of asbestos has been prohibited since the early 1990s, so it is reasonable to predict that the incidence of MPM will peak around the year 2020. By the year 2030 it is estimated that MPM will have caused approx. 250 000 deaths in Western Europe (Sohrab and Konietzko 2002). MPM has a very poor prognosis with a median survival time of 4–18 months. The average 5-year survival rate is no more than 2.5% (Bonomo et al. 2000).

MPM typically spreads within the pleural cavity. Accordingly, a hemorrhagic effusion is almost invariably present. It is also common for MPM to invade the chest wall, diaphragm, or mediastinum. Because MPM usually arises from cells of the parietal pleura, the pattern of nodal metastasis differs from that of parenchymal lung tumors. Initial nodal metastasis is usually to lymph nodes that drain the parietal pleura (TNM stage N2). Distant metastases are rare. The staging of MPM is based on the TNM classification (Rusch 1996).

The three histologic types of MPM are described as epithelial, mesenchymal, and mixed. The differentiated epithelial type is the most common and has, relatively, the best prognosis (Sugarbaker et al. 1999).

FDG PET is not useful for the T staging of MPM.

Imaging Studies

CT

The utility of PET-CT in MPM is still uncertain.

Typical findings. Typical morphologic features of MPM on CT scans are complete encasement of the lung or multiple sites of nodular pleural thickening with involvement of the interlobar septa. The tumor usually shows intense, inhomogeneous enhancement after intravenous contrast administration. Additionally, a pleural effusion is usually present, and pericardial effusion may develop in advanced cases. Often these signs are absent in the early stage, making it initially impossible to distinguish between a benign and a malignant pleural process on the basis of CT findings (Benamore et al. 2005).

In the early stage of MPM, it is often impossible to judge on the basis of CT whether the lesion is benign or malignant.

Staging. CT is the dominant imaging modality for the preoperative staging of MPM and supplies information that is essential for this purpose. Chest-wall invasion, pulmonary involvement (by lymphatic or hematogenous dissemination of tumor cells), and involvement of the pericardium and mediastinal lymph nodes can be adequately evaluated by CT. As with lung cancer, unequivocal CT signs of chest-wall or mediastinal invasion are bone destruction and/or invasion of the intercostal muscles. The obliteration of extrapleural fat planes is another manifestation of chest-wall involvement (Benamore et al. 2005). In one study, morphologic CT criteria were applied in 34 patients with MPM to correctly exclude chest-wall invasion in 93%, diaphragmatic invasion in 94%, and mediastinal invasion in 100% of the cases. The extent of chest-wall and diaphragmatic involvement was underestimated by CT, however (Patz et al. 1992).

FDG PET

Malignant pleural mesotheliomas show increased FDG uptake. Twenty-eight patients were evaluated by FDG PET imaging (Bénard et al. 1998). When a SUV cutoff of 2 was used, a sensitivity of 91% and a specificity of 100% were achieved in differentiating between malignant and benign pleural lesions. Epithelial MPM showed lower FDG uptake on average than the other types. The survival times of the seven patients who died from MPM showed a significant correlation with the mean SUV of the tumor (Bénard et al. 1999).

Other studies have also documented the contribution of FDG PET to the evaluation of pleural lesions (Carretta et al. 2000; Schneider et al. 2000). As in the case of CT, however, it is difficult to distinguish between MPM and a pleural metastasis from a nonpleural primary tumor (Carretta et al. 2000). It is essential, therefore, that the diagnosis be confirmed by biopsy before any treatment is initiated. Furthermore, FDG PET cannot provide accurate anatomic localization of increased uptake, making it unsuitable for T staging. In summary, the importance of FDG PET in the diagnosis and follow-up of MPM has not yet been fully established.

PET-CT

Available data on the utility of PET-CT in MPM are still inconclusive. Twenty-nine patients with MPM who were initially judged to be candidates for extrapulmonary pneumonectomy were evaluated by CT and FDG PET. In 11 of the patients the imaging results negated the indication for pneumonectomy. In 21 of the 29 patients the tumor was correctly staged by PET-CT (Erasmus et al. 2005). In another study, PET-CT was more accurate than PET and CT separately in establishing an indication for extrapulmonary pneumonectomy (Steinert et al. 2005).

PET-CT also provides useful information for evaluating lymph node status. Nodal status was correctly determined in 6 of 17 patients by PET-CT (Erasmus et al. 2005; **Fig. 2.30**).

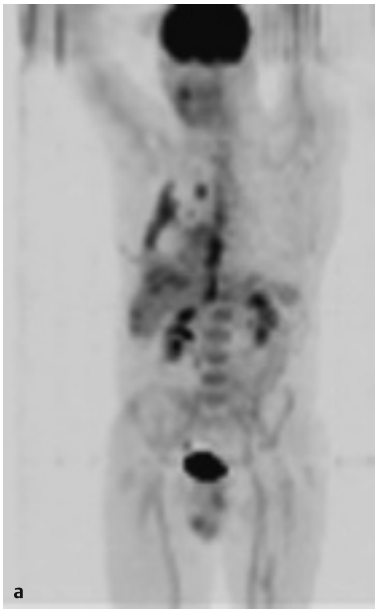

Fig. 2.30 a–g **Malignant pleural mesothelioma of the right hemithorax in a 63-year-old man.**

a FDG PET (MIP).

b–e PET-CT (**c, e**) with corresponding unenhanced low-dose CT scans (**b, d**). Nodular foci of pleural thickening show a combination of low FDG uptake (**c**, white arrow) and higher uptake (**c**, black arrow; **e**, white arrow). PET-CT is more accurate in determining the exact location of a hypermetabolic lesion for percutaneous biopsy. Enlarged mediastinal lymph node with a fatty hilum (**c**, gray arrow). Absence of FDG uptake indicates an inflammatory-reactive pathogenesis.

f, g Coronal reformations of FDG PET (**f**) and PET-CT (**g**). Accurate image fusion is technically difficult for lesions near the diaphragm (**g**, black and white arrows) but is easy for lesions distant from the diaphragm (**g**, gray arrow).

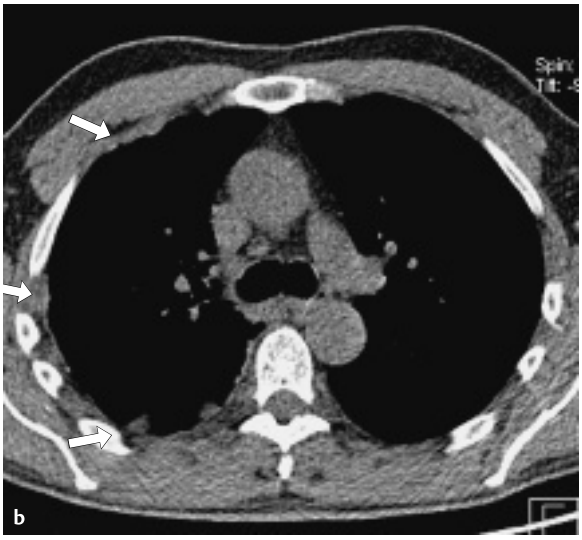

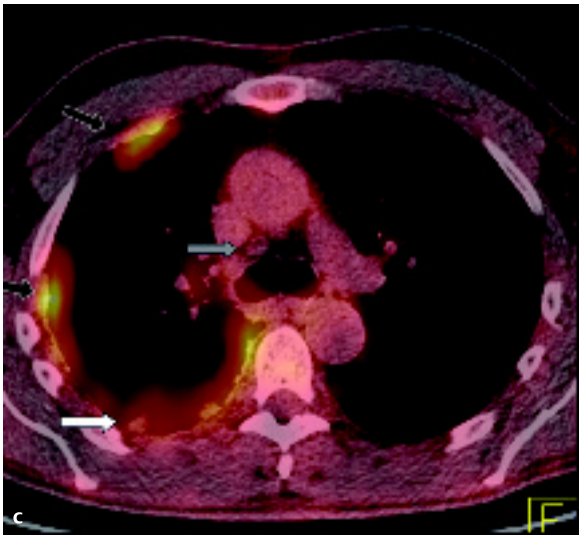

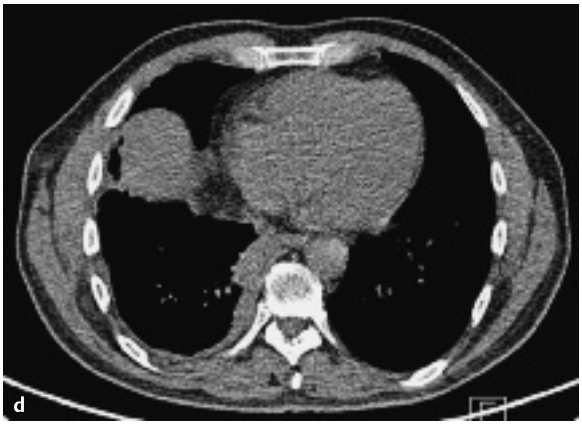

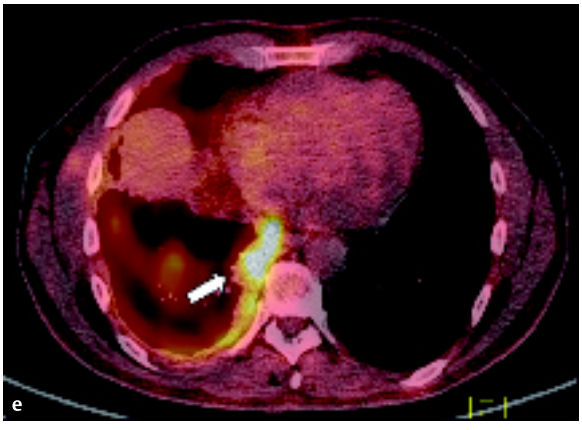

Continued →

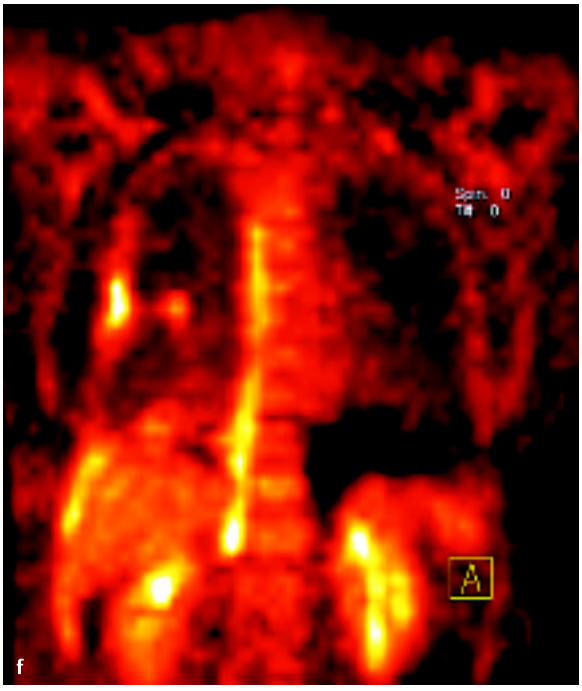

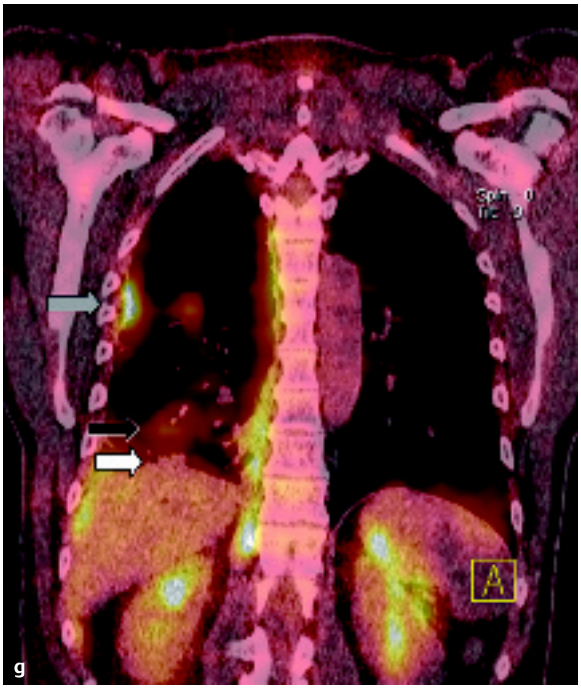

Fig. 2.30 a–g **Continued** (see legend on p. 115)

To date there have been no systematic studies on the accuracy of PET-CT for TNM staging compared with CT or FDG PET alone.

The combination of anatomic (CT) and metabolic (PET) information can also improve the accuracy of percutaneous biopsy (**Fig. 2.30**). This has clinical relevance because the cytologic evaluation of a pleural effusion or the histologic examination of a suspect lesion does not always yield definitive results, creating a need for multiple biopsies that may cause iatrogenic tumor cell dissemination (Boutin et al. 1995).

The respiratory movements of the diaphragm mean that there is a natural limit on the detection of diaphragmatic invasion by PET-CT. Early tumor involvement may be completely obscured by respiratory motion. In addition, variations in respiratory excursions may hamper the coregistration of FDG PET and CT images (**Fig. 2.30**).

Even CT may fail to detect a diaphragmatic tumor, because of the respiratory movements of the diaphragm.

Pulmonary Metastases

The lung is the most frequent target site for hematogenous metastasis from extrapulmonary malignancies. The tumors that most commonly metastasize to the lung are carcinomas of the thyroid gland, breast, and prostate, bone and soft-tissue sarcomas, and tumors of the testes, kidneys, adrenal glands, uterus, ovaries, and nasopharynx. Metastases account for the highest percentage of malignant pulmonary nodules.

CT

CT is the modality of choice for diagnosing pulmonary metastases, although lesions less than 6 mm in diameter are notoriously difficult to detect. A study on the detection of histologically confirmed pulmonary metastases by CT indicated an overall sensitivity of 77% for lesions of all sizes. The sensitivity was 94% for metastases 6–10 mm in size but 100% for metastases larger than 10 mm (Diederich et al. 1999).

Moreover, CT cannot positively distinguish between metastases and pulmonary nodules due to other causes. The size of a pulmonary nodule is of only limited value for determining whether or not it is malignant. The same is true of other morphologic parameters (Diederich et al. 2005). The pulmonary nodules detected by CT are frequently benign, even in patients with a known neoplastic disease (Kronawitter et al. 1999; Picci et al. 2001).

The accuracy of CT for identifying malignancy of a lesion can be increased by conducting follow-ups (analyzing changes over time) or by using CT with complementary modalities such as FDG PET.

FDG PET

The ability of FDG PET to detect pulmonary metastases has not yet been investigated for all primary tumor types. Nevertheless, studies to date indicate that FDG PET can detect pulmonary metastases from numerous primary extrapulmonary malignancies such as colon and breast cancer, malignant melanoma, and soft-tissue sarcomas

Steinert HC, Hauser M, Allemann F, et al. Non-small cell lung cancer: nodal staging with FDG PET versus CT with correlative lymph node mapping and sampling. Radiology 1997;202(2):441–446
Steinert HC, Santos Dellea MM, Burger C, Stahel R. Therapy response evaluation in malignant pleural mesothelioma with integrated PET-CT imaging. Lung Cancer 2005;49(Suppl 1):S33–S35
Strauss LG. Fluorine-18 deoxyglucose and false-positive results: a major problem in the diagnostics of oncological patients. Eur J Nucl Med 1996;23(10):1409–1415
Sugarbaker DJ, Flores RM, Jaklitsch MT, et al. Resection margins, extrapleural nodal status, and cell type determine postoperative long-term survival in trimodality therapy of malignant pleural mesothelioma: results in 183 patients. J Thorac Cardiovasc Surg 1999;117(1):54–63, discussion 63–65
Swensen SJ, Brown LR, Colby TV, Weaver AL, Midthun DE. Lung nodule enhancement at CT: prospective findings. Radiology 1996;201(2):447–455
Thomas M. Therapy of bronchial carcinoma: interdisciplinary and with expertise [in German]. Pneumologie 2002;56(2):90–93
Toloza EM, Harpole L, McCrory DC. Noninvasive staging of non-small cell lung cancer: a review of the current evidence. Chest 2003; 123(1 Suppl):137S–146S
Truong MT, Erasmus JJ, Macapinlac HA, et al. Integrated positron emission tomography/computed tomography in patients with non-small cell lung cancer: normal variants and pitfalls. J Comput Assist Tomogr 2005;29(2):205–209
Tyczynski JE, Bray F, Parkin DM. Lung cancer in Europe in 2000: epidemiology, prevention, and early detection. Lancet Oncol 2003;4(1):45–55
Vansteenkiste JF, Stroobants SG, De Leyn PR, et al. Lymph node staging in non-small-cell lung cancer with FDG-PET scan: a prospective study on 690 lymph node stations from 68 patients. J Clin Oncol 1998;16(6):2142–2149
Verschakelen JA, Bogaert J, De Wever W. Computed tomography in staging for lung cancer. Eur Respir J Suppl 2002;35:40s–48s
Virgo KS, McKirgan LW, Caputo MC, et al. Post-treatment management options for patients with lung cancer. Ann Surg 1995;222(6):700–710
von Schulthess GK, Steinert HC, Hany TF. Integrated PET/CT: current applications and future directions. Radiology 2006;238(2):405–422
Webb WR, Gatsonis C, Zerhouni EA, et al. CT and MR imaging in staging non-small cell bronchogenic carcinoma: report of the Radiologic Diagnostic Oncology Group.·. Radiology 1991;178(3):705–713
Weder W, Schmid RA, Bruchhaus H, Hillinger S, von Schulthess GK, Steinert HC. Detection of extrathoracic metastases by positron emission tomography in lung cancer. Ann Thorac Surg 1998;66(3):886–892, discussion 892–893
Wormanns D, Diederich S. Characterization of small pulmonary nodules by CT. Eur Radiol 2004;14(8):1380–1391
Wormanns D, Klotz E, Kohl G, et al. Enhancement measurement of pulmonary nodules with multirow detector CT: precision assessment of a 3D algorithm compared to standard procedure. Proc SPIE 2003;5032:795–801
Wright G, Manser RL, Byrnes G, Hart D, Campbell DA. Surgery for non-small cell lung cancer: systematic review and meta-analysis of randomised controlled trials. Thorax 2006;61(7):597–603
Yasufuku K, Fujisawa T. Staging and diagnosis of non-small cell lung cancer: invasive modalities. Respirology 2007;12(2):173–183
Yi CA, Lee KS, Kim BT, et al. Tissue characterization of solitary pulmonary nodule: comparative study between helical dynamic CT and integrated PET/CT. J Nucl Med 2006;47(3):443–450

B. Riemann
K. U. Juergens

Tumors of the Upper Digestive Tract

Esophageal Carcinoma

Most esophageal malignancies are diagnosed between 50 and 60 years of age, with males predominating in a 4:1 ratio. The physiologic constrictions of the esophagus are sites of predilection for esophageal carcinoma. Approximately 50% of cases present clinically in the middle third of the esophagus (constricted by the aortic arch and left main bronchus at the T4 level), while 35% present in the distal third (at the esophageal aperture of the diaphragm).

Esophageal carcinoma undergoes early lymphogenous metastasis.

Two histologic types of esophageal carcinoma are distinguished:

- Squamous cell carcinoma (≥95% of cases, **Fig. 2.31**), which occurs predominantly in the middle and upper thirds of the esophagus.
- Adenocarcinoma (approx. 4% of cases, **Fig. 2.32**), which occurs in the distal esophagus and at the gastroesophageal junction. This tumor is associated with Barrett syndrome (columnar epithelium lining the lower esophagus).

The CT criteria for a gastric malignancy are circumscribed wall thickening and an intraluminal mass.

Accurate tumor staging and the determination of histologic tumor type are essential in treatment planning for esophageal carcinoma.

Staging

The extent of esophageal carcinoma is described with the TNM classification, where T indicates the depth of tumor invasion, N describes lymph node status, and M denotes the presence or absence of distant metastasis.

Routes of metastasis. Because the esophagus lacks a serosal covering, esophageal cancer often undergoes early submucous spread at the cervical and thoracic levels. Even early stages show clinical evidence of lymphogenous spread to paraesophageal, mediastinal, cervical, and perigastric regional lymph nodes (stage N1).

Spread to celiac lymph nodes or supraclavicular sentinel nodes is classified as distant metastasis (stage M1).

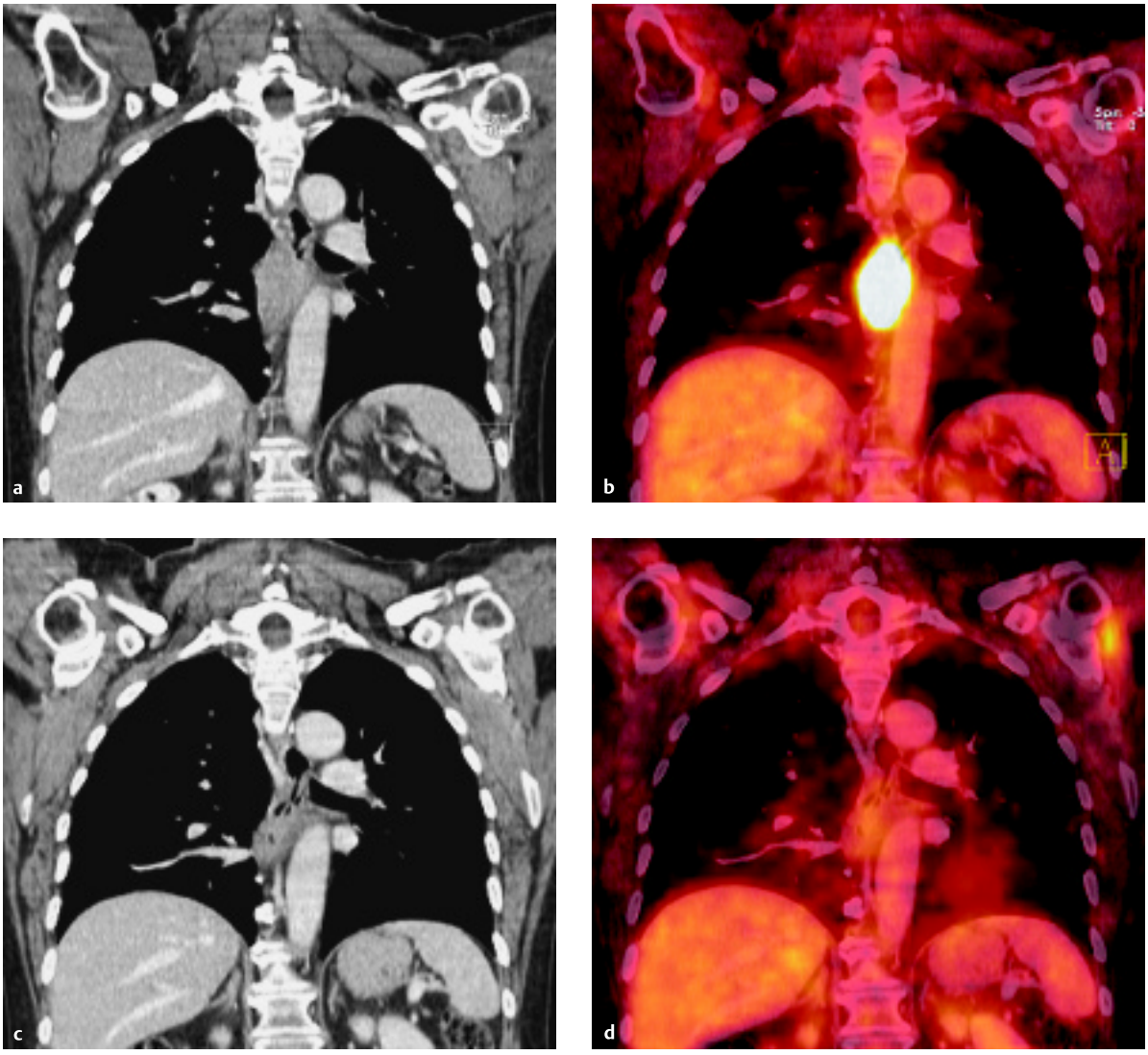

Fig. 2.31 a–d **Squamous cell carcinoma of the middle third of the esophagus in a 63-year-old man** (stage: uT3, N-positive). Follow-up study. CT (**a, c**) and FDG PET-CT (**b, d**) before treatment and after completion of the first cycle of neoadjuvant chemotherapy (cisplatin/5-FU). The SUV was reduced from 22.5 (**b**) to 4.8 (**d**). Final stage after esophageal resection: ypT0N0.

Imaging studies. Diagnostic imaging during preoperative staging provides a basis for deciding among several treatment options: radical excision with curative intent, neoadjuvant therapy, or a palliative approach. The gold standard for initial diagnosis is endoscopic examination and biopsy. Endoscopy permits a reliable evaluation of the mucosa, but the depth of tumor invasion into the esophageal wall cannot be accurately assessed. This has led to greater reliance on the combined use of esophagogastroduodenoscopy (EGD) and endosonography, although this method has limited application in patients with strictures and stenoses.

CT. The goal of primary staging is to ascertain the preoperative extent of disease as an aid to planning neoadjuvant therapy or defining the radiotherapy field. Multislice spiral CT is used for this purpose. This procedure can evaluate possible tumor invasion of adjacent organs (stage T4)—especially the tracheal wall, bronchi, pericardium, and aorta—as well as lymphogenous and hematogenous metastasis. The following CT signs are considered definitive for the invasion of adjacent organs:

- Obliteration of the paraesophageal fat plane
- More than 90° encasement of the aortic circumference
- Airway displacement or compression with intraluminal convexity
- Tracheoesophageal or bronchoesophageal fistula
- Cortical erosion of vertebral bodies

CT is used mainly for the determination of tumor extent.

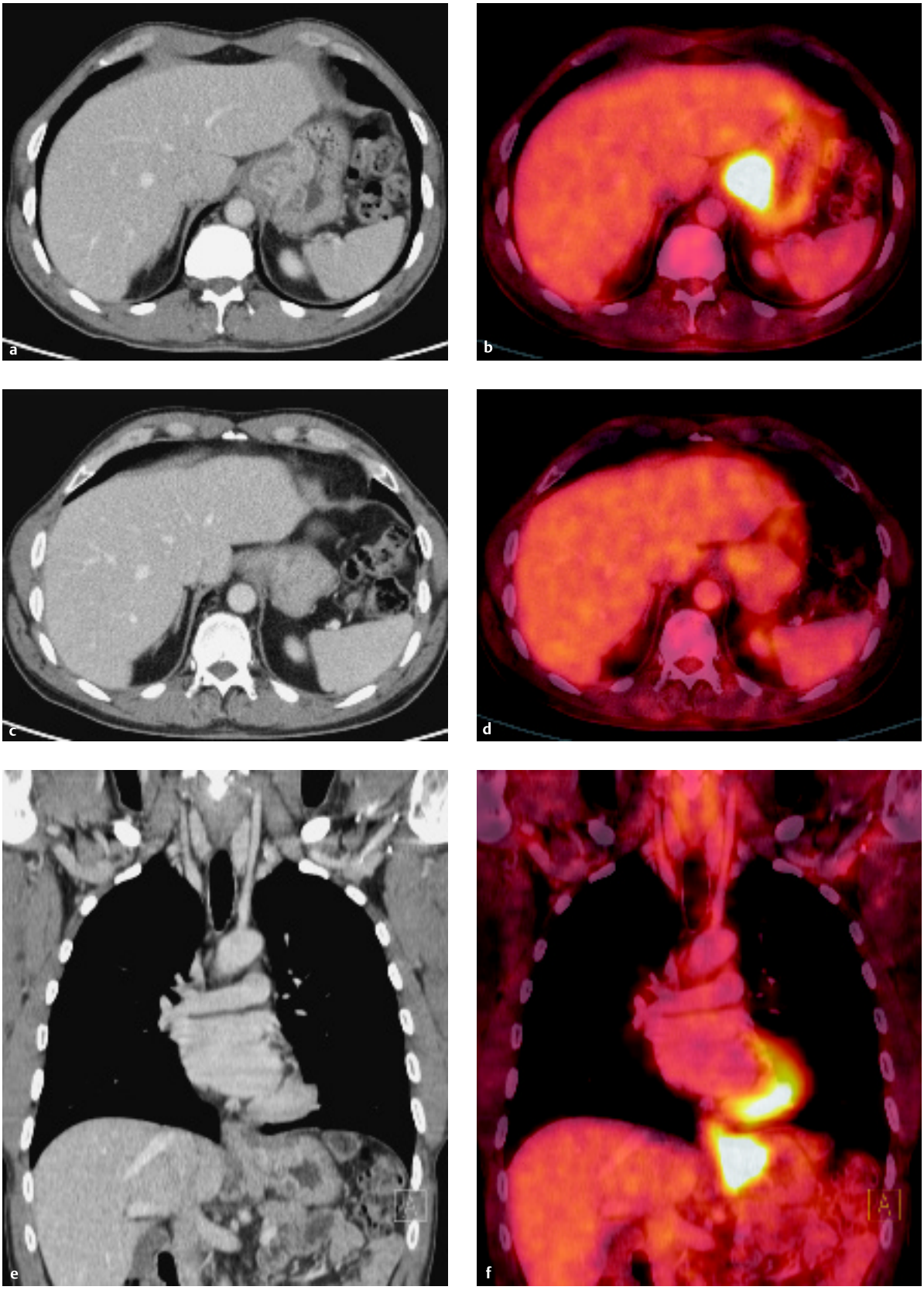

Fig. 2.32 a–h **Adenocarcinoma of the gastroesophageal junction in a 50-year-old man** (stage: uT3, N-positive). Follow-up study. CT and FDG PET-CT before treatment (**a, b, e, f**) and after completion of the first cycle of neoadjuvant chemotherapy (cisplatin/5-FU; **c, d, g, h**). The SUV was reduced from 17.3 to 3.5. Final stage after esophageal resection: ypT0N0.

Continued →

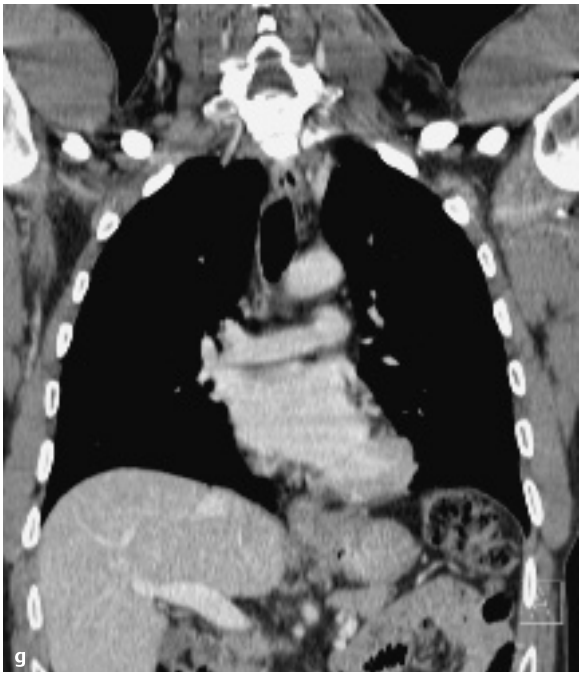

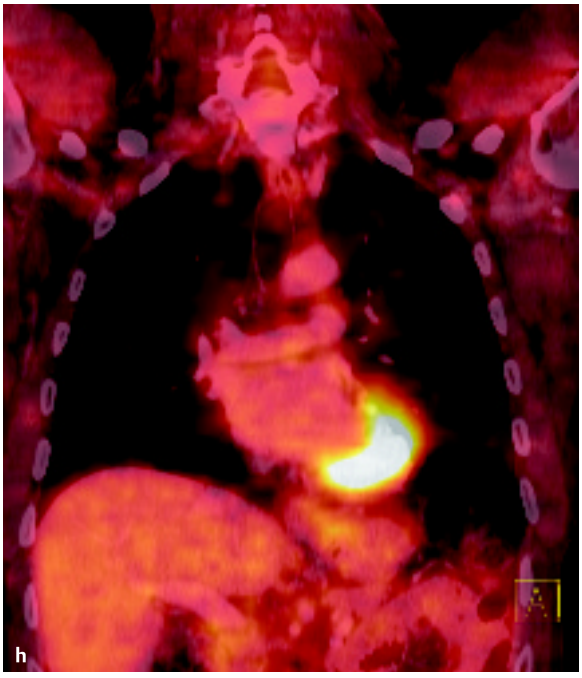

Fig. 2.32 a–g **Continued** (see legend on page 122)

Enlargement of paraesophageal or infradiaphragmatic lymph nodes to more than 8 mm is considered evidence of lymphogenous metastasis.

T staging with PET. In several studies, FDG PET has shown a high sensitivity (95%) and specificity (>90%) in the initial evaluation of squamous cell carcinoma and adenocarcinoma of the esophagus (Luketich et al. 1997; Block et al. 1997; Kole et al. 1998; McAteer et al. 1999; Kim et al. 2001; Kato et al. 2002). Most false-negative findings in these studies resulted from very small lesions that were below the 3- to 5-mm spatial resolution limit of PET imaging. No correlation has been found between the intensity of FDG uptake and the depth of tumor invasion in the esophageal wall (Fukunaga et al. 1998; Flamen et al. 2000).

FDG PET and CT have comparable sensitivity in the staging of esophageal cancer (Block et al. 1997; Kim et al. 2001). Due to difficulties in the anatomic correlation of PET findings, however, PET cannot add to the information supplied by endosonography in the assessment of wall invasion.

N staging with PET. The detection of locoregional lymph node metastases (N staging) has considerable prognostic importance. Contrast-enhanced CT is sensitive for this indication but has limited specificity. PET has 100% specificity for the N staging of esophageal carcinoma, but its sensitivity is only 45% (Luketich et al. 1997). The spatial resolution of conventional PET scanners is insufficient to positively distinguish locoregional lymph node metastasis from primary tumor involvement. Peripheral lymph nodes can be more accurately identified, however.

In recent studies, [^{18}F]FDG PET has been combined with [^{11}C]choline PET to permit the more accurate evaluation of mediastinal lymph nodes. To date, however, this combination has not yielded a diagnostic gain: the sensitivity of [^{18}F]FDG PET was 100% compared with 73% for [^{11}C]choline PET (Jager et al. 2001). This question has not yet been investigated by prospective studies in large groups of patients.

M staging with PET. The detection of distant metastases from esophageal carcinoma (M staging) is a critical factor in determining whether or not surgery is indicated. Patients with nodal or organ metastases have a poor prognosis that would contraindicate a radical excision with its attendant risks and morbidity. In patients with no evidence of distant metastases, the locoregional lymph node status determines the prognosis (**Figs. 2.33** and **2.34**).

FDG PET has a sensitivity of 69% and a specificity of 93% in the identification of distant metastases (Luketich et al. 1999), compared with only 46% and 74%, respectively, for CT. Even when compared with CT plus endosonography, FDG PET showed a higher sensitivity of 78% (vs. 46%) and a specificity of 90% vs. 69%; Lerut et al. 2000). The additional information supplied by FDG PET over morphologic imaging can influence treatment planning (Chatterton et al. 2009). This prompted the Third German Interdisciplinary Consensus Conference, titled "Onco-Pet III," to give FDG PET a class 1a indication (es-

FDG PET is superior to CT (even combined with endosonography) in the identification of distant metastases.

Prognosis

Conventional Imaging

Even dynamic contrast-enhanced MRI after preoperative chemotherapy cannot yet give an accurate prediction of lasting tumor remission (Reddick et al. 2001).

FDG PET

With osteosarcoma, the initial FDG uptake of the primary tumor is a prognostic indicator (Franzius et al. 2002b). Intense glucose hypermetabolism is associated with a reduction of overall and disease-free survival. This is consistent with the result of a large study in more than 200 adults and children with bone and soft-tissue sarcomas (Eary et al. 2002).

A prospective study of Ewing tumors demonstrated the prognostic value of glucose metabolism following neoadjuvant chemotherapy. In this study, too, high FDG uptake correlated with a shorter period of disease-free survival (Hawkins et al. 2005).

PET-CT

No studies have yet been published on the prognostic capabilities of PET-CT in patients with primary bone tumors.

Soft-Tissue Sarcomas

Basic Considerations

Soft-tissue sarcomas in children are a heterogeneous group of malignant tumors that originate in the soft tissues and have a predominantly mesenchymal origin. The most common histologic entities in children and adolescents are rhabdomyosarcoma (embryonal and alveolar, 61%), extraosseous Ewing sarcoma and peripheral neuroectodermal tumor (PNET, 8%), synovial sarcoma, neurofibrosarcoma, fibrosarcoma, and leiomyosarcoma (Kaatsch and Spix 2006). There is no uniform system for the staging and risk grouping of soft-tissue sarcomas. Pretreatment biopsy is always necessary. The diagnosis of soft-tissue sarcoma is based on morphologic and immunohistochemical criteria. The 10-year survival rate is 60% (Kaatsch and Spix 2006).

Conventional Imaging

Ultrasonography is often the initial imaging study for soft-tissue sarcomas, depending on lesion location and accessibility. Other sectional imaging studies are needed for evaluation of tumor extent, however. MRI provides significantly better soft-tissue contrast, does not involve ionizing radiation exposure, and is therefore preferred over other modalities. Pretreatment staging should also include chest radiographs in two planes, thoracic CT, cranial MRI, and abdominal ultrasonography or MRI (Gadner et al. 2006; AWMF 2007).

PET and PET-CT

No clinical studies have yet been published on the evaluation of pediatric soft-tissue sarcomas with FDG PET and PET-CT. In one series in which PET-CT was used in three patients with rhabdomyosarcoma it was concluded that slight FDG uptake in lymph nodes requires biopsy confirmation as it may indicate either metastasis or nonspecific activity (Ben Arush et al. 2006). In another series of four patients with rhabdomyosarcoma it was concluded that FDG PET is useful for evaluating response to therapy (Peng et al. 2006).

The great majority of soft-tissue sarcomas in children show intense glucose hypermetabolism (**Figs. 2.82, 2.83, 2.84, 2.85, 2.86, 2.87**). It is reasonable to conclude, then, that FDG PET is clinically useful for staging and for evaluating treatment response. Two larger studies of soft-tissue sarcomas in adults and some children have shown that FDG PET is not useful for the exclusion of pulmonary metastases, analogous to the results with bone sarcomas (Lucas et al. 1998; Iagaru et al. 2006). In cases where PET is proposed for staging, it would definitely be advantageous to obtain simultaneous CT images on a PET-CT scanner (**Fig. 2.88**)

Neuroblastoma

Basic Considerations

Neuroblastoma is the most common solid extracranial malignant tumor in children. Its incidence is 1.1:100 000 children under 15 years of age (Kaatsch and Spix 2006). As an embryonal tumor, neuroblastoma is most frequently diagnosed in infants and small children. It originates from cells of the neural crest and thus occurs predominantly in the sympathetic trunk, paraganglia, and adrenal medulla. Tumors of the sympathetic nervous system show increased catecholamine production in more than 80% of patients.

Staging is based on the International Neuroblastoma Staging System (INSS). Stage IV, characterized by the presence of distant metastasis, has a particularly grave prognosis. Molecular genetic characteristics also have prognostic significance (e.g., N-*myc* amplification). The 10-year survival rate is 53% for all patients but varies

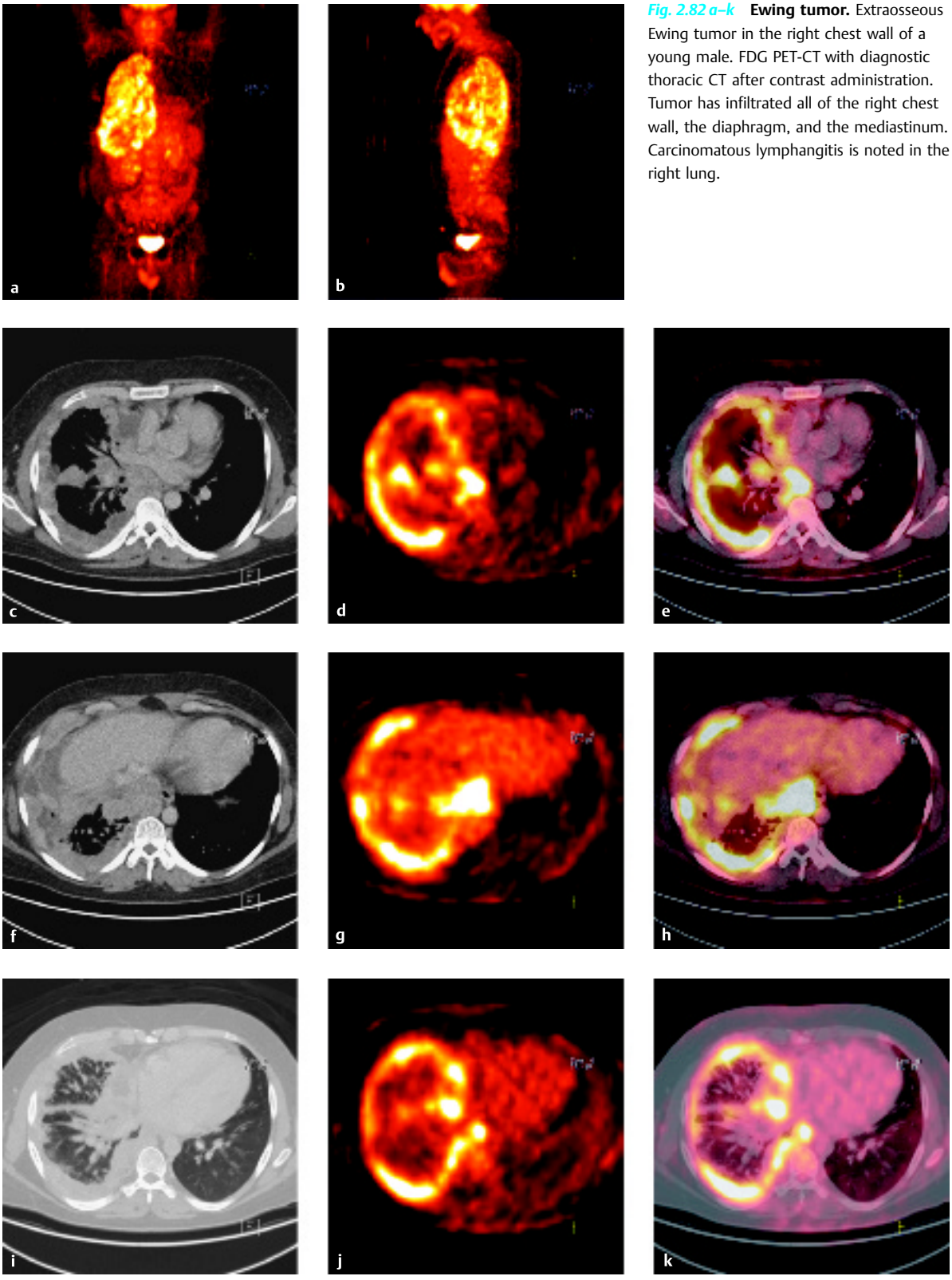

Fig. 2.82 a–k **Ewing tumor.** Extraosseous Ewing tumor in the right chest wall of a young male. FDG PET-CT with diagnostic thoracic CT after contrast administration. Tumor has infiltrated all of the right chest wall, the diaphragm, and the mediastinum. Carcinomatous lymphangitis is noted in the right lung.

a FDG PET, coronal whole-body MIP.
b FDG PET, sagittal whole-body MIP.
c–h Axial scans of the chest at two different levels (**c, f** CT with a soft-tissue window; **d, g** FDG PET, **e, h** PET-CT).
i–k Axial scan through the chest (**i** CT with a lung window, **j** FDG PET, **k** PET-CT).

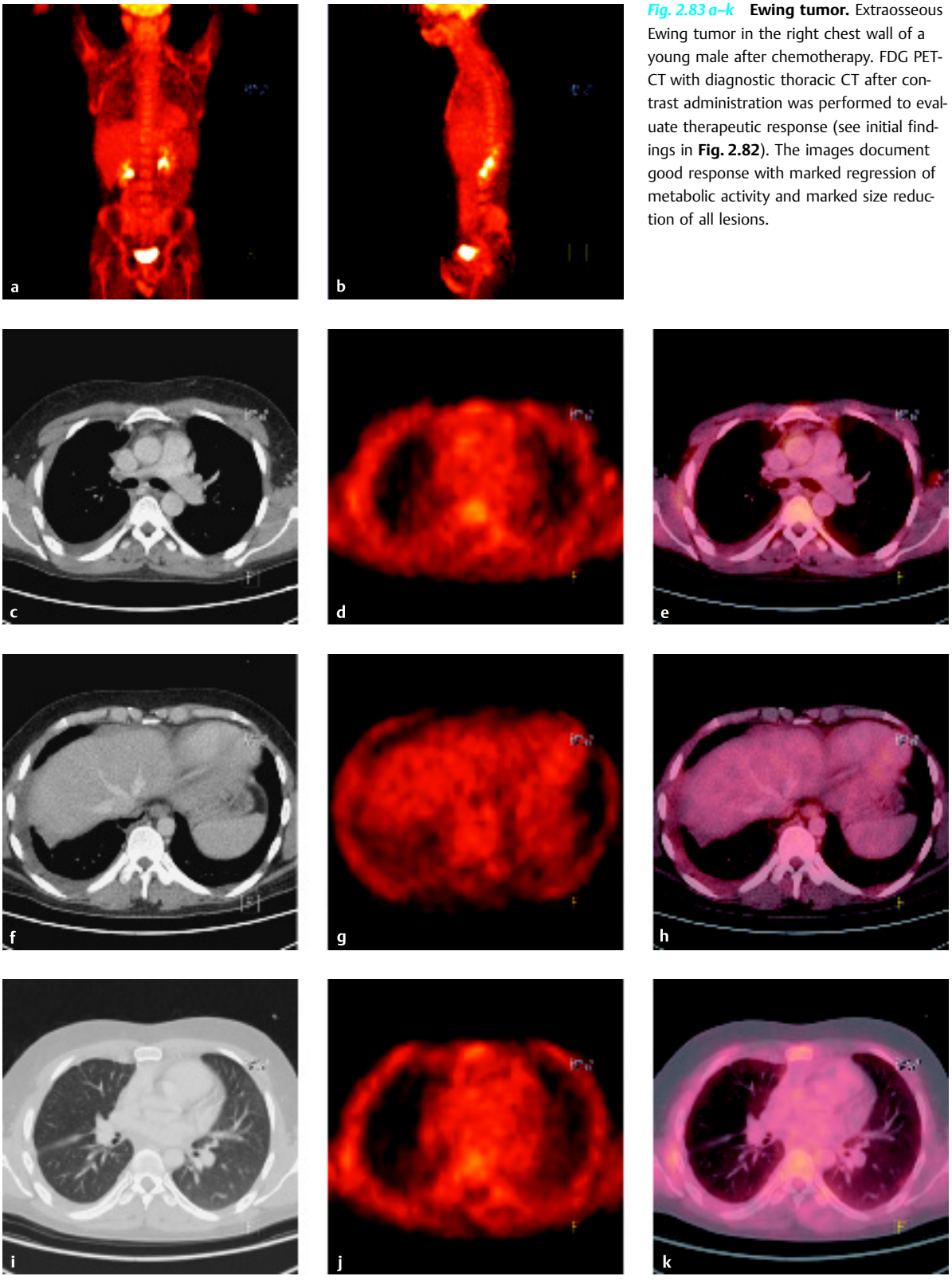

Fig. 2.83 a–k **Ewing tumor.** Extraosseous Ewing tumor in the right chest wall of a young male after chemotherapy. FDG PET-CT with diagnostic thoracic CT after contrast administration was performed to evaluate therapeutic response (see initial findings in **Fig. 2.82**). The images document good response with marked regression of metabolic activity and marked size reduction of all lesions.

a FDG PET, coronal whole-body MIP.
b FDG PET, sagittal whole-body MIP.
c–h Axial scans of the chest at two different levels (**c, f** CT with a soft-tissue window; **d, g** FDG PET; **e, h** PET-CT).
i–k Axial scan through the chest (**i** CT with a lung window, **j** FDG-PET, **k** PET-CT).

Index

D

E

F

O

P

Q

R

U

V

W

X